Macroscopic motion of liquid metal plasma facing components in a diverted plasma

M. A. Jaworski[a,*], S. P. Gerhardt[a], N. B. Morley[b], T. Abrams[a], R. Kaita[a], J. Kallman[a], H. Kugel[a], R. Majeski[a], and D. N. Ruzic[c]

[a] *Princeton Plasma Physics Laboratory, Princeton, NJ, 08543, USA*

[b] *MAE Department, University of California, Los Angeles, CA 90095-1597, USA*

[c] *University of Illinois at Urbana-Champaign, 104 S. Wright St., Urbana IL 61801, USA*

Abstract

Liquid metal plasma facing components (PFCs) have been identified as an alternative material for fusion plasma experiments. The use of a liquid conductor where significant magnetic fields are present is considered risky, with the possibility of macroscopic fluid motion and possible ejection into the plasma core. Analysis is carried out on thermoelectric magnetohydrodynamic (TEMHD) forces caused by temperature gradients in the liquid-container system itself in addition to scrape-off-layer currents interacting with the PFC from a diverted plasma. Capillary effects at the liquid-container interface will be examined which govern droplet ejection criteria. Stability of the interface is determined using linear stability methods.

In addition to application to liquid metal PFCs, thin film liquid metal effects have application to current and future devices where off-normal events may liquefy portions of the first wall and other plasma facing components.

PACS: 47.56.+r, 44.30.+v

JNM Keywords: First wall materials, lithium, liquid metals

PSI-19 Keywords: Divertor Material, Liquid metals, SOL Current, plasma facing component, Liquid Lithium

Corresponding author address: USA

Corresponding author email: mjaworsk@pppl.gov

Presenting author: Michael A. Jaworski

Presenting author e-mail: mjaworsk@pppl.gov

1 Introduction

Plasma-facing components (PFCs) must meet increasingly difficult machine conditions. The combination of increased machine power and pulse length creates large energies deposited onto the materials, as well as high particle fluences. These large heat and particle loads result in sputtering erosion and significant thermal gradients. A recent report to the Fusion Energy Science Advisory Committee, known as the "Greenwald" report[1] highlighted the issues facing solid components with respect to component lifetime and long-term damage. One alternative to solid components is the use of liquid metal plasma-facing components (LMPFCs)[2].

Liquid metals present possible solutions even as they provide new challenges such as unintended motion of the liquid metal. In the case of the DIII-D DiMES probe, a liquid lithium sample 1mm deep and 25mm in diameter was ejected into the plasma[3]. In order to arrest the liquid against motion, mesh based porous systems have been used[4] with success on several machines[5, 6]. The usage of a high-surface area structure is used to create a liquid which is dominated by surface tension forces. Such capillary systems can also exhibit unexpected motion such as droplet ejection[7]. Contrasting these results is that of the CDX-U machine which implemented an open tray of liquid lithium[8]. In this apparatus, careful implementation of the tray was utilized to mitigate currents that would eject the lithium, although motion was observed to be still possible during e-beam heating[9].

Recent experimental work with liquid lithium has reported a new result which informs on additional sources of current. The demonstration of thermoelectric magnetohydrodynamic (TEMHD) pumping has been achieved at the University of Illinois in the Solid/Liquid Lithium Divertor Experiment(SLiDE)[10]. In brief, thermoelectric currents arise in the liquid metal and container walls, these currents react with the external magnetic field and create a body force in the liquid; it is this body force that creates motion in the liquid. TEMHD occurs without external current inputs and only requires a liquid and solid pair with differing Seebeck coefficients, a temperature gradient along the material interface, and a magnetic field. This difference in Seebeck coefficient can even occur between the phases of the same material (*e.g.* between the liquid and solid). It was found that TEMHD will dominate the dynamics of liquid lithium melts in many systems over thermocapillary effects. This pumping effect may have implications for

the power handling capability of the liquid metal[11] and the results of this effect on the stability of fluid films is the subject of the present work.

In addition to currents induced in the PFC, currents from the scrape-off-layer (SOL) can drive motion. The currents have been observed on several machines and are often caused by plasma temperature gradients[12]. Along with these plasma thermoelectric currents, disruptions can cause large currents to flow through PFCs (so called halo currents) and within them (eddy currents).

Although the present analysis will use properties of liquid lithium for example calculations and estimates (due to its relevance toward NSTX), the equations here developed are applicable to other materials provided the appropriate databases are available.

2 Currents Within the PFC

Currents entering the PFC are divided into two classes: machine-linked and PFC-linked. Figure 1 indicates the difference between the two. That is, machine-linked currents pass through the PFC and re-enter the plasma at another location. Examples include parallel temperature-gradient thermoelectric scrape-off-layer currents(SOLC)[13] and halo currents arising from bulk plasma motion. PFC-linked currents pass through the PFC material only and re-enter the plasma. Examples of this include eddy currents arising from rapid plasma current changes and motion[14] and cross-field plasma current sources such as perpendicular temperature-gradient thermoelectric currents[12].

[Figure 1 about here.]

In order to begin assessment of the plasma currents arising from these several effects in NSTX, a set of Langmuir probes have been deployed in the machine[15] with electronics capable of measuring both types of current[16]. Machine-linked currents are determined directly by measuring the current collected by a grounded probe tip. PFC-linked currents are determined directly by measuring the current passing through two probe-tips at different locations in the plasma. Figure 2 shows measurements of the machine-linked currents in a 900 kA, 2 MW NBI, ELM-free discharge in NSTX. The strike point sweeps over the inner two probes at about 0.5

s and was was held nominally held at the set-point location after this time. The measurements indicate significant spatial gradients in SOLC in the vicinity of the strike-point and a typical magnitude is of order 10–20 $\mathrm{kA/m^2}$. Figure 2 also shws initial measurement of the PFC-linked SOLC in NSTX. The two probes were initial set at the same radial location with a toroidal gap of 500 $\mu\mathrm{m}$ for testing during two 900 kA discharges with the strike point approximately 10 cm inboard of the probe location. In order to demonstrate that a real current was being measured, the toroidal order of the two probe tips was reversed and the measured current reversed as well. Detailed study of the source of this current is planned for future work.

[Figure 2 about here.]

3 Thermoelectric Material Currents

The thermoelectric effect operating between the liquid layer and the solid substrate also creates a current within the PFC[17, 10]. The current resulting in the liquid metal under the conditions for TE current listed above is give as:

$$j_{\mathrm{TEMHD}} = \frac{\sigma P \nabla T_i}{C+1} \tag{1}$$

where j_{TEMHD} is the current density, σ is the liquid electrical conductivity, P is the thermoelectric power of the liquid-solid pair, ∇T_i is the temperature gradient along the interface between the material pair, and h is the liquid thickness. The variable $C = \sigma h/(\sigma_w t_w)$ represents the non-dimensional impedance ratio between liquid and solid where σ_w and t_w are the electrical conductivity and thickness of the solid, respectively.

4 Expected Motion from Currents

As the two current paths are orthogonal, one would expect very different behavior from each. For example, in a horizontal divertor target the machine-linked currents are z-directed. Magnetic field is approximated as being purely tangential to the PFC surface. The primary gradient in material temperature, and plasma temperatures, are in the radial direction. As a result, the

PFC linked currents are R-directed. The resulting Lorentz force from the machine-linked currents is then along the surface of PFC and for the PFC-linked currents, in the vertical direction.

In the case of lateral forces along the PFC surface, the velocity of the liquid can be estimated from the Navier-Stokes equation for a conducting fluid[18]. The solution to lateral flow maximum, u_0, caused by an incident current density is given as follows:

$$u_0 = \frac{j_s}{\sigma B}\left[1 - \frac{1}{\cosh(\mathrm{Ha})}\right] \tag{2}$$

where $\mathrm{Ha} = hB\sqrt{\sigma/\mu}$ is the Hartmann number, j_s is the current density, B is the magnetic field, h is the fluid depth, σ is the fluid electrical conductivity and μ is the dynamic viscosity. For reference, the liquid lithium layer in the NSTX Liquid Lithium Divertor(LLD) is of order 1 $\mu\mathrm{m}$ on the porous surfaces[19]. For layers of this thickness, the expected velocity is less than 100 $\mu\mathrm{m/s}$ for an incident current density of 20 $\mathrm{kA/m^2}$.

In the case of vertical forces there is the possibility of droplet ejection. The governing instability in this situation is the Raleigh-Taylor instability as there is a body force accelerating the fluid away from a stagnant equilibrium configuration. The solution for a magnetized fluid under the destabilizing influence of gravity is a long studied problem and we simply cite Chandrasekhar's work on the topic of fluid instabilities[18]. The imposed current is separated from the MHD generated currents such that the resulting acceleration is $jB/\rho - g$ for an upward directed Lorentz force and the normal mode perturbation follows $exp(ik_x x + ik_y y + nt)$ and here treating the plate as a Cartesian system with x and y representing the toroidal and radial directions, respectively. k_x and k_y are the wave numbers of the perturbation in these directions and n is the growth rate. Following with the derivation in [18], the resulting growth rate for the instability is given as follows:

$$n^2 = k(jB/\rho - g)\left[1 - \frac{k^2\Sigma}{(jB/\rho - g)\rho} - \frac{B^2 k_x^2}{2\pi\mu_0(jB/\rho - g)\rho k}\right] \tag{3}$$

where μ_0 is the permeability of vacuum, Σ is the surface tension and $k = \sqrt{k_x^2 + k_y^2}$. From the normal mode definition above, values of n which are real are unstable and grow exponentially. Imaginary values of n result in oscillatory solutions and are stable. Here, the influence of surface

tension and magnetic field can be seen to stabilize against instability by driving the value of $n^2 < 0$. The most unstable mode occurs when the wave vector is oriented perpendicular to the magnetic field ($k_x = 0$) and this is considered in the following analysis.

Equation 3 can be re-arranged to determine the critical wave number, k_{Cr}, of the system (for the least stable mode) by setting the group within the $[\cdots]$ equal to zero. The solution is given as follows:

$$k_{Cr} = \sqrt{\frac{jB - \rho g}{\Sigma}} \tag{4}$$

Making use of eq. 1 in eq. 4, the critical wavenumber as a function of temperature gradient for a given liquid-container pair can be calculated and is shown in Fig. 3 for the case of a lithium layer on top of a 10 mm thick molybdenum substrate.

[Figure 3 about here.]

As the linear stability theory can only provide information about the modes and associated growth rates near equilibrium, additional information is needed to provide limits on which k are likely to result. This information often comes from geometric considerations, such as the container radius or a mean pore size, for instance. In the case of a semi-infinte flat plate with a thin layer of liquid, however, there are no nearby features on which to rely. To overcome this limitation, we propose a simple non-linear model for the resulting droplet.

[Figure 4 about here.]

Figure 4 shows a diagram of the droplet. The critical point of the droplet is defined by the static force balance of the droplet given as:

$$\rho(jB/\rho - g)V_{\mathrm{drop}} = 2\pi R_{\mathrm{drop}}\Sigma\cos\theta \tag{5}$$

where V_{drop} is the droplet volume, R_{drop} is the droplet radius and θ is the contact angle of the droplet side walls. The surface tension force is maximized when the contact angle zero and this represents a half-sphere droplet. The solution is assumed to be periodic, similar to the linear stability theory and mass is assumed to be conserved in the periodic domain. That is, an original

disk of material of thickness, h, and radius $2R$ transitions into a droplet on top of a thinned disk of thickness, δ given as follows:

$$\frac{1}{2}\left(\frac{4}{3}\pi R^3\right) + \pi(2R)^2\delta = \pi(2R)^2 h \tag{6}$$

which, solving for the maximum droplet radius (at $\delta = 0$) provides $R_{drop} = 6h$.

In order to achieve initial thinning or "necking" and eventual ejection from the surface, the net body force must exceed the surface tension at the critical point. Solving eq. 5 for the critical current density after non-linear growth gives the following criteria:

$$j_{\mathrm{crit,NL}} = \frac{\rho g}{B}\left(\frac{3\Sigma}{\rho R^2 g + 1} + 1\right) \tag{7}$$

Or, in the case of a thermoelectric current source, the resulting critical temperature gradient is given as follows:

$$\nabla T_{\mathrm{i,crit,NL}} = (C' + 1)\frac{\rho g}{\sigma P B}\left(\frac{3\Sigma}{\rho R^2 g} + 1\right) \tag{8}$$

where $C' = \sigma(h + R)/(\sigma_w t_w)$ is the adjusted dimensionless impedance accounting for the droplet growth. Figure 5 shows the critical current density for a range of droplet radii and equivalent fluid depths according to the non-linear estimate.

[Figure 5 about here.]

5 Discussion

In both the linear stability analysis and non-linear droplet ejection, the critical current densities increase as the fluid depth decreases. A simple estimate for temperature gradient can be made by assuming 1D conduction through the substrate material such that $\nabla T_i \approx L/k\nabla q$. Temperature gradients of order $10^3\ \mathrm{K/m}$ could be expected for a molybdenum substrate and incident heat flux gradients of 100 $\mathrm{MW/(m^2 - m)}$, typical of the NSTX divertor[20]. For these temperature gradients the TE current density would approach the 100 $\mathrm{kA/m^2}$ level which exceeds the quiescent SOLCs measured to date.

For the LLD in NSTX, the present fill thickness is not expected to have exceeded 10 μm.

At such thin liquid levels, very large current densities would be required to produce significant motion laterally or to create instability. To date, no droplet formation or ejection has been observed which is consistent with the present work.

For the case of the CDX-U tray, no droplet ejection was observed during plasma discharges, though this tray was $5\ \mathrm{mm}$ thick and would be less stable to ejection. The typical shot length in CDX-U was less than 100 ms and this amount of time is a factor of 10 less than the thermal diffusion time, τ, through $5\ \mathrm{mm}$ of liquid lithium ($\tau \approx h^2/\alpha \approx 1\ \mathrm{s}$ where α is the thermal diffusivity).

Despite these null results, an experimental investigation would strengthen the theories developed here. The existence of TE currents as demonstrated in [10] could strongly alter the motion of liquid lithium layers, and for materials which have discontinuous Seebeck coefficients at phase change, could alter the motion of melt layers in solid PFCs that undergo anomalous heating from the plasma (*e.g.* a runaway electron beam).

6 Conclusion

The motion of liquid metal plasma facing components under interaction with divertor plasmas is analyzed. SOLC are divided into machine- and PFC-linked currents which result in orthogonal motion of the liquid metal. In addition to currents entering from the plasma, thermoelectric effects between the liquid and solid substrate will also create currents when temperature gradients are present. PFC-linked currents in the radial direction will be capable of producing vertically destabilizing forces. Linear stability theory utilizing these external Lorentz forces is provided indicating when the fluid layer will go unstable. A simple non-linear model is provided to estimate the maximum droplet radii for thin-layers of fluid. Critical current densities and, in the case of TE generated currents, critical temperature gradients, are developed. In all cases, thin layers are more resistant to motion and this is consistent with observations made in NSTX to date.

Acknowledgments

This work is supported under the U.S. Department of Energy contract #DE-AC02-09CHI1466.

References

[1] M. Greenwald, *et al.*, Tech. rep., Fusion Energy Sciences Advisory Committee (October 2006).

[2] M. A. Abdou, *et al.*, Fusion Engineering and Design 54 (2) (2001) 181–247.

[3] D. G. Whyte, *et al.*, Fusion Engineering and Design 72 (2004) 133–147.

[4] V. A. Evtikhin, *et al.*, Fusion Engineering and Design 49–50 (2000) 195–199.

[5] V. A. Evtikhin, *et al.*, Plasma Physics and Controlled Fusion 44 (2002) 955–977.

[6] M. L. Apicella, *et al.*, Journal of Nuclear Materials 363–365 (2007) 1346–1351.

[7] G. Y. Antar, *et al.*, Fusion Engineering and Design 60 (2002) 157–166.

[8] R. Majeski, *et al.*, Journal of Nuclear Materials 313–316 (2003) 625–629.

[9] R. Kaita, *et al.*, Physics of Plasmas 14 (2007) 056111.

[10] M. A. Jaworski, *et al.*, Phys. Rev. Lett. 104 (2010) 094503.

[11] M. A. Jaworski, N. B. Morley, D. N. Ruzic, Journal of Nuclear Materials 390–391 (2009) 1055–1058.

[12] P. C. Stangeby, The Plasma Boundary of Magnetic Fusion Devices, Institute of Physics Publishing, 2000.

[13] A. Kumagai, *et al.*, Plasma Phys. Control. Fusion 39 (1997) 1189–1196.

[14] S. P. Gerhardt, J. E. Menard, Nucl. Fusion 49 (2009) 025005.

[15] J. Kallman, *et al.*, Rev. Sci. Instrum.Submitted.

[16] M. A. Jaworski, *et al.*, Rev. Sci. Instrum.Submitted.

[17] J. A. Shercliff, Journal of Fluid Mechanics 91 (1979) 231–251.

[18] S. Chandrasekhar, Hydrodynamic and Hydromagnetic Stability, Dover Publications, Inc., New York, 1961.

[19] H. Kugel, *et al.*, Fus. Eng. Des. 84 (2009) 1125–1129.

[20] V. A. Soukhanovskii, *et al.*, Journal of Nuclear Materials 337–339 (2005) 475–479.

List of Figures

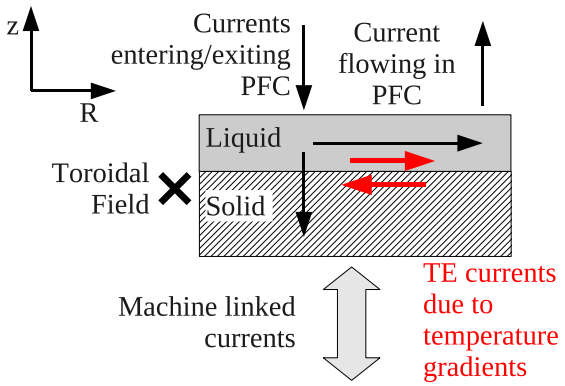

Figure 1: Cartoon indicating currents interacting with the liquid metal layer. Arrows indicate current flow.

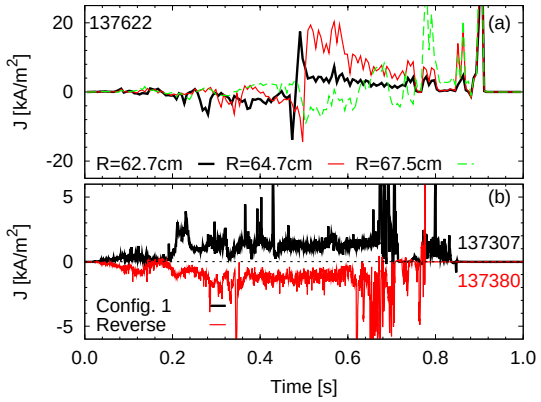

Figure 2: Measurements of (a) machine-linked and (b) PFC-linked SOLC in NSTX. In (a), the strike point sweeps over the inner two probes at about 0.5 s. In (b), two similar discharges are compared with the probe configuration reversed to confirm the signal is reliable. Data has been smoothed for readability.

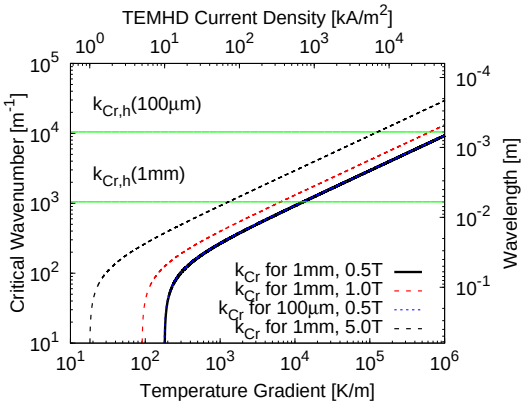

Figure 3: Critical wavenumber for a given temperature gradient for a Li layer on a 10 mm thick molybdenum substrate. Lines labeled $k_{Cr,h}$ indicate limiting wavenumbers from the non-linear model. Equivalent wavelength, $\lambda = 2\pi/k$ is also given for reference. Wavenumbers below (or wavelengths above) the critical wavenumber are unstable.

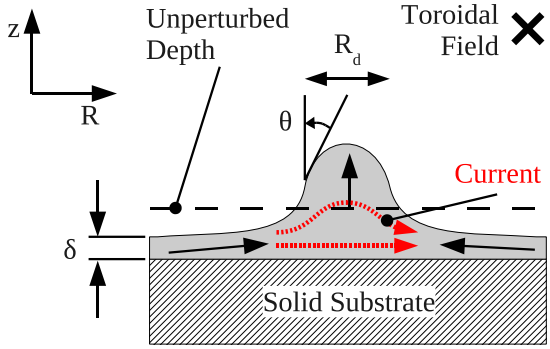

Figure 4: Diagram of droplet after non-linear growth period.

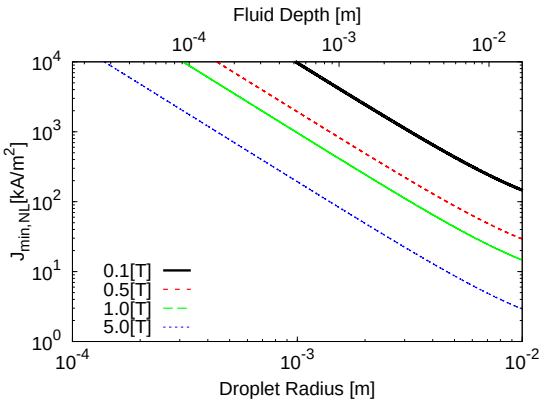

Figure 5: Critical current density for ejection of a droplet after the non-linear growth of a droplet of liquid lithium.